# OBSERVER INDEPENDENT MEASURES OF SNOW INSTABILITY

Benjamin Reuter*, Alec van Herwijnen, Jürg Schweizer

WSL Institute for Snow and Avalanche Research SLF, Davos, Switzerland

ABSTRACT: Observer independent measures of snow instability are a prerequisite for modeling, verifying and improving avalanche forecasts. However, presently no metrics directly related to snow instability exist. Instead, signs of instability or results from snow instability tests are frequently used to assess instability or the avalanche danger. Whereas these observations are well related to instability, they are subjective and difficult to use for quantitative analyses. We therefore developed three metrics of snow instability inspired by our understanding of the avalanche release process. We used a data set of over a hundred snow micro-penetrometer resistance profiles and concurrently performed propagation saw tests and rutschblock tests to model, in a first step, failure initiation and crack propagation with finite elements. A stress-based criterion and an estimate of the critical cut length as obtained with a PST were derived from the force signal of the SMP measurements. While both instability measures agreed well with observed signs of instability, some discrepancies were observed. We therefore introduced a third criterion based on modeled tensile stresses in the slab in comparison with the strength of the slab layers. Preliminary results indicate that with this three-step approach snow instability can be derived with observer-independent metrics related to the avalanche release processes. The criteria refer to failure initiation and the onset of crack propagation and are complemented with a tensile failure criterion related to the phase of dynamic crack propagation.

KEYWORDS: snow instability, avalanche forecasting, snow micro-penetrometer, avalanche initiation, crack propagation, tensile strength, finite element modeling

## 1. INTRODUCTION

Improving avalanche forecasts, whether conventional or numerical, requires verification. Without verifying the predictions of snow instability in space and time (McClung 2000) one cannot evaluate when and where the forecast was correct. However, there is presently no metric that describes snow instability – and even less so avalanche danger (Föhn and Schweizer 1995). Even in hindsight a correct assessment of avalanche danger is impossible and burdened by observer biases (Techel et al. 2016).

In the absence of a directly measurable quantity, indicators of instability such as recent avalanches, whumpfs or shooting cracks (Jamieson et al. 2009) are used to estimate snow instability. Often these signs are not observed and in their absence, performing snow instability tests (Schweizer and Jamieson 2010) is considered the method of choice. Alternatively, the temporal evolution of snow stability can be monitored by calculating stability indices from weak layer shear frame tests (Jamieson et al. 2007; Roch 1966a, 1966b).

With traditional field tests, information at the snowpack or 'pit' scale are obtained, but for estimating avalanche hazard the slope or basin scale should be considered (for a definition of scales see Schweizer and Kronholm 2007). This scale mismatch (Hägeli and McClung 2004) can only be overcome with multiple measurements and/or modelling approaches. To this end, a metric amenable to quantitative analyses and suited for recording multiple measurements is required; thus, classical manual observation methods and stability tests do not qualify.

An obvious candidate for providing quantitative, observer independent measures of snowpack properties is the snow micro-penetrometer (SMP; Schneebeli and Johnson 1998). Indeed, the SMP penetration resistance has been related to snow instability (e.g., Bellaire et al. 2009; Pielmeier and Schweizer 2007; Schweizer and Reuter 2015). However, these attempts do not consider the first two, most essential stages of dry-snow slab avalanche release: failure initiation and crack propagation (Schweizer et al. 2016).

In need of a measurement technique of snow instability, but also with the idea of a future ap-

* *Corresponding author address:*
Benjamin Reuter, WSL Institute for Snow and Avalanche Research SLF, Flüelastrasse 11, CH-7260 Davos Dorf, Switzerland.
email: reuter@slf.ch

proach combining snow cover modeling and fracture mechanical concepts, we developed metrics of snow instability from observer independent snowpack measurements using the SMP.

In the following, we describe how snow mechanical properties are measured with the snow micro-penetrometer, we define the metrics and apply our approach to a data set including field observations of snow instability. As the metrics are based on the above mentioned fracture processes preceding avalanche release, it becomes clearer how 'snow instability' is controlled by these processes.

## 2. METHODS

### 2.1 Field data set

From routine measurements and field campaigns during the winter seasons between 2003 and 2015 we accumulated a field data set containing 147 measurements with the snow micro-penetrometer (SMP) and corresponding observations of snow stratigraphy and snow instability. The data were all collected around Davos (Eastern Swiss Alps) and contain detailed manually observed snow profiles (Fierz et al. 2008) showing the primary weakness and all slab layers above. The SMP measurements were performed in close vicinity to the profiles providing signals of penetration resistance to a depth well below the weak layer. In 55 cases a propagation saw test (PST; Gauthier and Jamieson 2006) and in 64 cases a Rutschblock test (RB; Föhn 1987) is available. In other words, we deal with two data sets: a PST and a RB data set, while apart from the tests, both data sets contain the same data. Furthermore, for all sampling days presence and type, or absence of signs of instability were recorded.

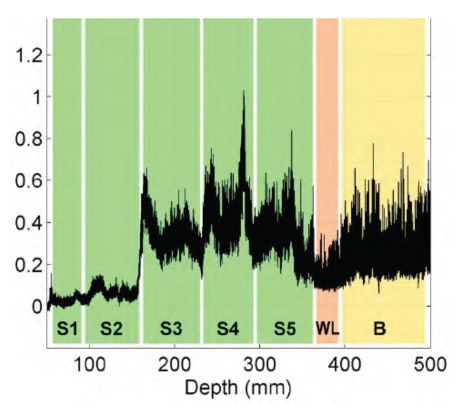


Fig. 1: Penetration resistance (black) measured with the SMP over snow depth. Five slab layers (green), a weak layer (orange) and a basal layer (yellow) were defined.

### 2.2 Snow mechanical properties

Based on the manually observed snow profile, layers were defined from the corresponding sections of the SMP signal, namely slab layers, a weak layer and a basal layer (Figure 1). As every layer is later represented in a finite element (FE) model and the resolution of the SMP is higher than required for FE simulations, we deal with layers for the sake of shorter computation times. Hence, every SMP signal was divided into up to 11 layers each having a thickness and separate snow mechanical properties.

From the SMP signal three microstructural parameters were extracted (Löwe and van Herwijnen 2012). They consisted of the rupture force $f$, the deflection at rupture $\delta$ and the structural element size $L$, calculated over a moving window $w$ of 2.5 mm with 50% overlap and then averaged across the layer. Following recent work, we derived the snow mechanical properties for every layer based on the microstructural parameters of this layer. Snow density was calculated after Proksch et al. (2015), micro-mechanical elastic modulus and strength $\sigma$ were calculated after Johnson and Schneebeli (1999), and the specific fracture energy and the penetration depth after Reuter et al. (2015a).

### 2.3 Modelling snow instability

A modeling approach based on the finite element method was used to calculate metrics related to failure initiation and crack propagation of a certain slab-weak layer system characterized by an SMP signal.

The strength-over-stress criterion $S = \frac{\sigma_{\mathrm{WL}}}{\Delta\tau}$ was calculated from the strength of the weak layer $\sigma_{\mathrm{WL}}$ derived from the SMP signal and the maximum additional shear stress at the depth of the weak layer $\Delta\tau$. The latter was obtained from a finite element simulation modelling the linear elastic behavior of the snow layers defined from the SMP signal under the load of a skier (Reuter et al. 2015a). Hence, the criterion $S$ estimates the propensity to failure initiation under skier loading.

The critical crack length $r_{\mathrm{c}}$ was determined by inverting an analytic expression for the specific fracture energy (Heierli et al. 2008; van Herwijnen et al. 2016) and solving for the snow mechanical properties derived from the SMP, except for the effective elastic modulus of the slab. It was modeled with the finite element method from the change of mechanical energy of the snow slab during bending, as it would be observed in a PST in the field (Reuter et al. 2015a). The critical crack length $r_c$ is a measure of the crack propagation propensity.

To complement the two above mentioned SMP-derived metrics of instability, we developed a third criterion, the tensile failure criterion, since during the initial state of dynamic crack propagation recent work suggests that the tensile strength of the slab might determine how far a running crack will propagate (Gaume et al. 2015b; Schweizer et al. 2014).

In order to model the tensile stresses in the slab at the onset of crack propagation we modeled the PST with finite elements. In the model each layer had the mechanical properties as derived from the SMP analysis. From the finite element solution the maximum tensile stress within each slab layer was calculated. The tensile strength was calculated from the SMP-derived snow layer density according to Jamieson and Johnston (1990). Hence, a tensile strength-over-stress criterion for every layer in the SMP signal was derived. To do so, the tensile strength in each slab layer was divided by the maximum tensile stress modeled with finite elements in the same layer. The thickness of all layers with values below a threshold of 0.5 were summed up and divided by the total slab thickness. This third metric is called tensile criterion $T_c$.

## 3. RESULTS

The first two metrics of snow instability were compared with snow instability tests, namely the RB score and the critical cut length as observed in the PST.

For the comparison with the RB score, we grouped scores 1 and 2 as well as 6 and 7 because scores 1 and 7 were rarely observed. The criterion $S$ increased with increasing RB score, best seen in the monotonic increase of the median of the failure initiation criterion (indicated by gray lines) per RB class (Figure 2). If for a given $S$ there was no overlap of the boxes, the predictive power of $S$ would obviously be very good. Although this is not the case, the monotonic increase is significant and is reflected in a high Spearman rank correlation coefficient ($r_s > 0.9$).

The modeled critical crack length was compared with the critical crack length observed in field experiments (Figure 3). Modeled and measured values of the critical crack length were related ($r_p = 0.61$).

Our field records also contain information about the observation of signs of instability allowing validating the modeled snow instability metrics with

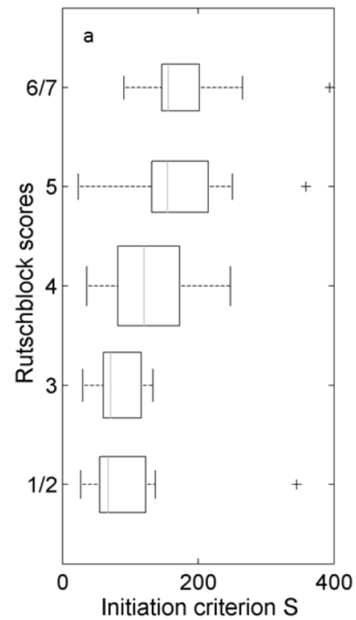


Fig. 2: Modeled failure initiation criterion $S$ vs. RB score (N = 64). Boxes span the interquartile range from 1st to 3rd quartile with a horizontal line showing the median (grey line). Widths of the boxes correspond to the number of cases. Whiskers extend to the most extreme data points not considered outliers (crosses) within 1.5 times the interquartile range above the 3rd and below the 1st quartile.

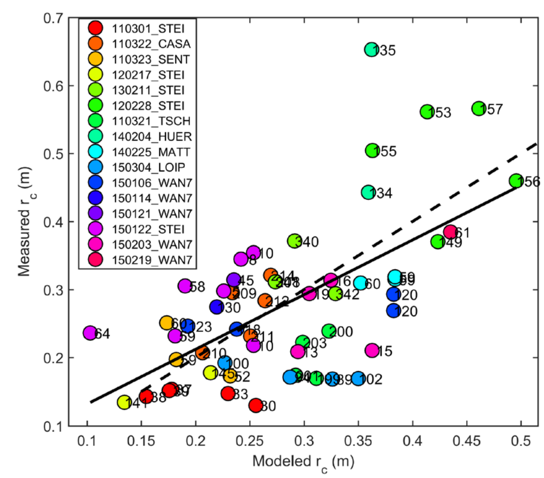


Fig. 3: Modeled and measured critical crack lengths $r_c$ are contrasted (N = 55). Experiments grouped by date and location with colors. Solid line shows linear regression, dashed line indicates the 1:1 line.

another independent observation. Those field observations were grouped into: whumpfs, shooting cracks with or without whumpfs (“cracks") or “all signs" (whumpfs, cracks and recent avalanches); i.e., fresh avalanches were only observed simultaneously with whumpfs and cracks. To jointly relate our modeled metrics of instability to the observations of instability we contrasted the propensity to crack propagation, i.e., modeled critical crack length $r_c$, and failure initiation, i.e., initiation criterion $S$, in Figure 4.

Signs of instability were primarily present in the lower left of Figure 4, i.e., for low values of the failure initiation criterion and the critical crack length. Vice versa no signs of instability were reported if both criteria yielded high values (upper right). This finding suggests that both criteria are required to assess snow instability.

Combining both snow instability criteria yielded a probability of detection for signs of instability of 100%; the proportion correct takes into account also the false alarm rate, and yielded 81%. In other words, a number of non-observations of signs of instability remain in the lower left quadrant of the graph (19 out of 57).

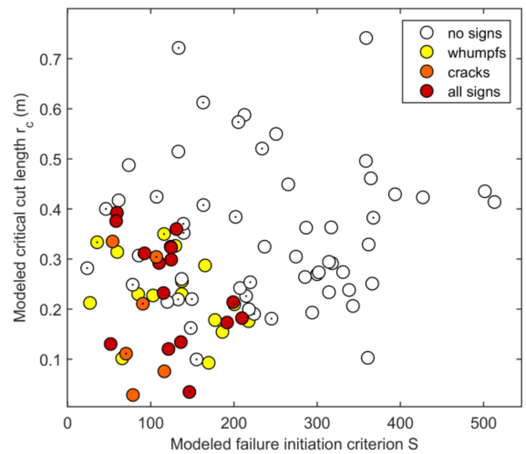


Fig. 4: Type and presence of signs of instability against failure initiation criterion $S$ and critical crack length $r_c$, both modeled. Colors indicate type of observed signs of instability (whumpfs, shooting cracks, all signs). Open circles indicate that no signs of instability were reported explicitly. Dots mark partially propagating fractures observed as slab fractures in PSTs or partial releases in Rutschblock tests.

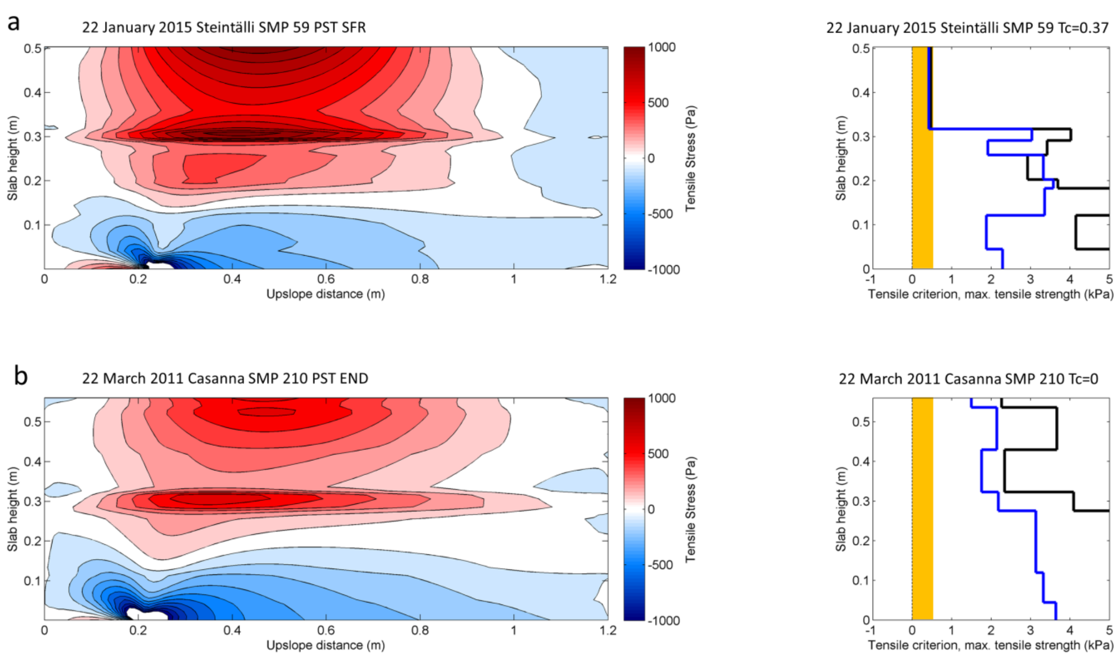


Fig. 5: Examples of the model results for a PST with (a) slab fracture and (b) with a crack propagating to the end of the column. (Left) The modeled tensile stress in the PSTs, in both cases, slope angle $\alpha = 0$, crack length $r_c = 0.23$ m. Positive stresses refer to tension (red), negative values to compression (blue). (Right) Profiles of the tensile strength of slab layers (blue) and the tensile criterion (black).The orange strip indicates the critical range below 0.5.

In fact, among those 19 data points, the ones coming from the PST data set, were many slab fractures (7), and the ones coming from the RB dataset were mostly partial releases (not "whole block"; 8). Finding still some only partially propagating cracks while both criteria were critical (lower left in Figure 4), we investigated the tensile behavior of the slab at the onset of crack propagation.

Figure 5 shows the tensile stresses in the slab layers due to bending of the snow beam at the onset of propagation for two PSTs, one with an observed slab fracture and one with a crack propagating to the end.

While cases with slab fractures had high values ($T_c > 0.3$) of the tensile criterion (e.g., Figure 5a), cases in which fractures propagated to the end had low values (e.g., Figure 5b). Hence, in the latter case, the sum of layer thickness of layers below the threshold of the strength-over-stress ratio of 0.5 was lower ($T_c < 0.15$). In many such cases (19 out of 33) not a single layer was in the critical range, yielding a value of $T_c = 0$. Hence, the criterion divided the group with slab fractures from the group with end results in PSTs (Figure 6a).

All cases with sign of instability had low values of the tensile criterion (Figure 6b and c). The tensile criterion split cases with signs of instability from cases without observed signs of instability at a split value of 0.25.

Combining all three metrics for the PST data set in order to predict signs of instability 8 out of the 9 cases without signs of instability within the critical range of the failure initiation and crack propagation criterion (lower left quadrant in Figure 4) could be explained by low values of the tensile criterion. Hence, including the third criterion considerably increased the classification accuracy.

## 4. DISCUSSION

To capture two important steps preceding the detachment of a snow slab, we used in a first approach two criteria, the failure initiation criterion $S$ and the critical crack size for self-propagation $r_c$. As the approach allows deriving both metrics from penetration resistance profiles measured with the snow micro-penetrometer, it represents the first method to obtain observer independent measures of snow instability. Until now traditional, manually observed snow profiles only provided indirect, mainly phenomenological observations hindering an estimation of the relevant physical properties, except for snow density or shear strength (e.g., Jamieson and Johnston 2001; Proksch et al. 2016).

Based on a comparison with signs of instability observed in the field during the sampling days the metrics for failure initiation and crack propagation have been validated. Only if both metrics were below a critical value, signs of instability were observed, in line with our understanding of the sequence of fractures preceding slab avalanche release.

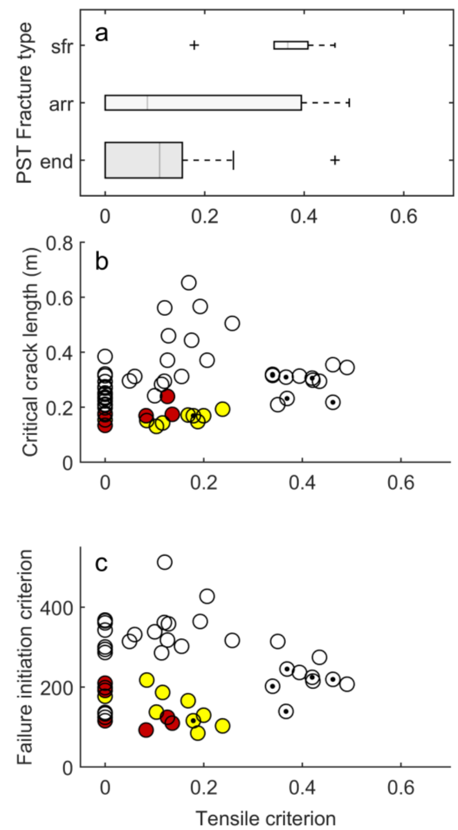


Figure 6: Tensile criterion, (a) versus PST fracture type (with classes "end" in 34 cases, "arrest" in 14 cases and "slab fracture" in 7 cases). Same boxplot representation as in Fig. 2; (b) versus the modeled failure initiation criterion and (c) the critical crack length; colored full circles denote signs of instability as in Fig. 4.

However, a number of situations remained when "unstable" conditions were expected based on these two metrics, but signs of instability were not observed. Following a simple approach to compare the tensile strength and the maximum tensile stress in the slab layers, we defined a new tensile criterion.

This approach was motivated by previous research on the reasons for slab tensile failure. Schweizer et al. (2014) analyzed a large PST data set and found low slab density to be an indicator for slab fractures in PSTs. In addition, Gaume et al. (2015a) found that for full slope releases a sufficient snow slab density is required. In other words, a certain tensile strength in the slab is needed for sustained propagation. However, Gaume et al. (2015a) also suggested that the tensile failure is a secondary process which is triggered by a locally stronger zone in the weak layer arresting crack propagation in the first place.

Including the third criterion increased the classification accuracy. However, we performed the analysis with the PST data set only, as only for this data set PST fracture types were available. In the future, we plan to extend the analysis to a larger data set including the RB data.

Assessing the performance of the model approach with two different field tests (RB and PST) yielded plausible results. However, the main source of uncertainty is related to the mechanical properties needed as input for the model.

In addition, the model itself has some uncertainty because the behavior of snow is not fully explained by linear elastic mechanics, although this assumption is usually satisfactory. Snow density, effective elastic modulus and specific fracture energy were all determined from SMP measurements. Uncertainties related to the determination of these mechanical properties are on the order of 10-20% at best (Reuter et al. 2013). Other known SMP error sources, such as signal drift due to strong temperature differences, were identified and those measurements discarded. Therefore, the scatter seen in the comparison of the snow instability metrics with the manual field tests is partly due to model and measurement uncertainties, but probably also stem from uncertainties involved with the field techniques.

## 5. CONCLUSIONS

We presented three observer-independent measures of snow instability based on measurements with the snow micro-penetrometer and validated the results with field observations. With a simple strength-over-stress criterion applied to the modeled tensile stresses in a PST the existing classification based on the failure initiation and the crack propagation criterion was enhanced. Preliminary results are promising, but the tensile criterion may need further validation with larger data sets.

These observer-independent metrics of snow instability pave the road towards snow instability estimation beyond the pit scale. The criteria can be derived from one penetration resistance signal measured with the SMP, which allows performing multiple penetration resistance profiles within a day. Hence, such distributed field data sets covering a small catchment can be used to study spatial variations of snow instability and investigate the influences of terrain or meteorological drivers (e.g., Reuter et al. 2016; Reuter et al. 2015b).

## ACKNOWLEDGEMENTS

We are grateful to many colleagues from SLF who helped with field work.

## REFERENCES

Bellaire, S., C. Pielmeier, M. Schneebeli, and J. Schweizer, 2009: Stability algorithm for snow micro-penetrometer measurements. *J. Glaciol.*, **55,** 805-813.

Fierz, C., and Coauthors, 2008: The 2008 international classification of seasonal snow on the ground. *Proceedings ISSW 2008, International Snow Science Workshop, Whistler, Canada, 21-27 September 2008*, C. Campbell, S. Conger, and P. Haegeli, Eds., 579-580.

Föhn, P. M. B., 1987: The Rutschblock as a practical tool for slope stability evaluation. *Symposium at Davos 1986 - Avalanche Formation, Movement and Effects, IAHS Publ., 162*, International Association of Hydrological Sciences, Wallingford, Oxfordshire, U.K., 223-228.

Föhn, P. M. B., and J. Schweizer, 1995: Verification of avalanche danger with respect to avalanche forecasting. *Les apports de la recherche scientifique à la sécurite neige, glace et avalanche. Actes de Colloque, Chamonix, 30 mai-3 juin 1995*, F. Sivardière, Ed., ANENA, 151-156.

Gaume, J., G. Chambon, N. Eckert, M. Naaim, and J. Schweizer, 2015a: Influence of weak layer heterogeneity and slab properties on slab tensile failure propensity and avalanche release area. *Cryosphere*, **9,** 795–804.

Gaume, J., A. van Herwijnen, G. Chambon, K. W. Birkeland, and J. Schweizer, 2015b: Modeling of crack propagation in weak snowpack layers using the discrete element method. *Cryosphere*, **9,** 1915-1932.

Gauthier, D., and J. B. Jamieson, 2006: Towards a field test for fracture propagation propensity in weak snowpack layers. *J. Glaciol.*, **52,** 164-168.

Hägeli, P., and D. M. McClung, 2004: Hierarchy theory as a conceptual framework for scale issues in avalanche forecasting modeling. *Ann. Glaciol.*, **38,** 209-214.

Heierli, J., P. Gumbsch, and M. Zaiser, 2008: Anticrack nucleation as triggering mechanism for snow slab avalanches. *Science*, **321,** 240-243.

Jamieson, B., P. Haegeli, and J. Schweizer, 2009: Field observations for estimating the local avalanche danger in the Columbia Mountains of Canada. *Cold Reg. Sci. Technol.*, **58,** 84-91.

Jamieson, J. B., and C. D. Johnston, 1990: In-situ tensile tests of snowpack layers. *J. Glaciol.*, **36,** 102-106.

Jamieson, J. B., and C. D. Johnston, 2001: Evaluation of the shear frame test for weak snowpack layers. *Ann. Glaciol.*, **32,** 59-68.

Jamieson, J. B., A. Zeidler, and C. Brown, 2007: Explanation and limitations of study plot stability indices for forecasting dry snow slab avalanches in surrounding terrain. *Cold Reg. Sci. Technol.*, **50,** 23-34.

Johnson, J. B., and M. Schneebeli, 1999: Characterizing the microstructural and micromechanical properties of snow. *Cold Reg. Sci. Technol.*, **30,** 91-100.

Löwe, H., and A. van Herwijnen, 2012: A Poisson shot noise model for micro-penetration of snow. *Cold Reg. Sci. Technol.*, **70,** 62-70.

McClung, D. M., 2000: Predictions in avalanche forecasting. *Ann. Glaciol.*, **31,** 377-381.

Pielmeier, C., and J. Schweizer, 2007: Snowpack stability information derived from the SnowMicroPen. *Cold Reg. Sci. Technol.*, **47,** 102-107.

Proksch, M., H. Löwe, and M. Schneebeli, 2015: Density, specific surface area and correlation length of snow measured by high-resolution penetrometry. *J. Geophys. Res.*, **120,** 346-362.

Proksch, M., N. Rutter, C. Fierz, and M. Schneebeli, 2016: Intercomparison of snow density measurements: bias, precision, and vertical resolution. *Cryosphere*, **10,** 371-384.

Reuter, B., J. Schweizer, and A. van Herwijnen, 2015a: A process-based approach to estimate point snow instability. *Cryosphere*, **9,** 837-847.

Reuter, B., B. Richter, and J. Schweizer, 2016: Snow instability patterns at the scale of a small basin. *J. Geophys. Res. Earth Surf.*, **121,** 257-282.

Reuter, B., A. van Herwijnen, J. Veitinger, and J. Schweizer, 2015b: Relating simple drivers to snow instability. *Cold Reg. Sci. Technol.*, **120,** 168-178.

Reuter, B., M. Proksch, H. Löwe, A. van Herwijnen, and J. Schweizer, 2013: On how to measure snow mechanical properties relevant to slab avalanche release. *Proceedings ISSW 2013. International Snow Science Workshop, Grenoble, France, 7-11 October 2013*, ANENA, IRSTEA, Météo-France, Grenoble, France, 7-11.

Roch, A., 1966a: Les déclenchements d'avalanches. *Symposium at Davos 1965 - Scientific Aspects of Snow and Ice Avalanches, IAHS Publication, 69*, Int. Assoc. Hydrol. Sci., 182-195.

Roch, A., 1966b: Les variations de la résistance de la neige. *Symposium at Davos 1965 - Scientific Aspects of Snow and Ice Avalanches, IAHS Publication, 69*, Int. Assoc. Hydrol. Sci., 86-99.

Schneebeli, M., and J. B. Johnson, 1998: A constant-speed penetrometer for high-resolution snow stratigraphy. *Ann. Glaciol.*, **26,** 107-111.

Schweizer, J., and K. Kronholm, 2007: Snow cover spatial variability at multiple scales: Characteristics of a layer of buried surface hoar. *Cold Reg. Sci. Technol.*, **47,** 207-223.

Schweizer, J., and J. B. Jamieson, 2010: Snowpack tests for assessing snow-slope instability. *Ann. Glaciol.*, **51,** 187-194.

Schweizer, J., and B. Reuter, 2015: A new index combining weak layer and slab properties for snow instability prediction. *Nat. Hazards Earth Syst. Sci.*, **15,** 109-118.

Schweizer, J., B. Reuter, A. van Herwijnen, and J. Gaume, 2016: Avalanche release 101. *Proceedings ISSW 2016. International Snow Science Workshop, Breckenridge CO, U.S.A., 3-7 October 2016*.

Schweizer, J., B. Reuter, A. van Herwijnen, J. B. Jamieson, and D. Gauthier, 2014: On how the tensile strength of the slab affects crack propagation propensity. *Proceedings ISSW 2014. International Snow Science Workshop, Banff, Alberta, Canada, 29 September - 3 October 2014*, 164-168.

Techel, F., L. Dürr, and J. Schweizer, 2016: Variations in individual danger level estimates within the same forecast region. *Proceedings ISSW 2016. International Snow Science Workshop, Breckenridge CO, U.S.A., 3-7 October 2016*.

van Herwijnen, A., J. Gaume, E. H. Bair, B. Reuter, K. W. Birkeland, and J. Schweizer, 2016: Estimating the effective elastic modulus and specific fracture energy of snowpack layers from field experiments. *J. Glaciol.*, 10.1017/jog.2016.90.